Soft Comput (2018) 22:1421–1432
https://doi.org/10.1007/s00500-017-2827-9

FOCUS

Early ramp warning using vehicle behavior analysis

Hua Cui[1] · Zefa Wei[1] · Xuan Wang[1] · Xinxin Song[1] · Pannong Li[1] · Huansheng Song[1] · Xiang Ma[1]

Published online: 13 September 2017

Abstract The ramp entrance connects the main road and the ramp and is the merging zone for vehicles from main road and ramp. As ramp entrance is considered to be the most accident-prone area, this paper focuses on the early warning to avoid collision of vehicles for the ramp entrance on freeway. Firstly, we studied the relation between the vehicle speed and collision risk by analyzing the vehicle trajectories. Secondly, the risk grades were defined based on the lag of the time when vehicles enter into the merging zone from the main road and the ramp. Finally, the risk grade was released by the information board and vehicle terminal to make driver aware of it, so that the vehicles can pass the merging zone in sequence rather than collide with each other. Theoretical analysis and experiment results show that the proposed method could realize early warning for the ramp entrance, reducing the possible traffic accidents.

Keywords Ramp entrance · Time lag · Risk grade · Collision warning · Vehicle trajectories

1 Introduction

For current highways, the merging of on-ramp vehicles can have an invasive influence on the main road traffic and is often a source of traffic congestion and oscillation (Bertini and Malik 2004; Yi and Mulinazzi 2007). Moreover, road traffic accident statistics reports demonstrate that the rate of vehicle collision accidents in the on-ramp merging areas of highways is higher than that in the other sections. According to statistics, about 30% of traffic accidents occur in ramp area every year in China. For instance, in a certain section of Shanghai to Ningbo freeway in China, traffic accidents that occurred in the on-ramp merging area account for 6% of the total accidents, and the accident rate of per km is about four times than that of the basic sections. The rate of traffic accidents on the Shenyang to Dalian freeway that happened in the entrance ramp is about 5.5% and the accident rate of per km is about 4.5 times than that of the basic sections (Zhang 2006), while in the USA, 20–30% of freeway truck accidents occur on or near ramps (Janson et al. 1998). On-ramp merging areas on a highway, e.g., the entrance or exit ramps, are characterized by the roads that are used to merge two traffic flows into one and can be considered as mandatory lane-changes. Side-scratch and rear-end collision are subject to happen in such scenarios. So, a proper merging control and management at the merging area is critically important for traffic safety and traffic flow improvement. In the past, a number of research outcomes to address traffic control and management at the merging areas have been published (Papageorgiou and Kotsialos 2002; Hajiahmadi et al. 2016; Muller et al. 2015; Chow et al. 2009; Li and Chow 2015; Lu et al. 2010; Park and Smith 2010; Shao et al. 2015; Abbas et al. 2013; Khoufi et al. 2014; Imai et al. 2014; Wang et al. 2013).

The most conventional approach to manage the merging traffic is ramp metering (RM) (Papageorgiou and Kotsialos 2002; Papageorgiou and Papamichail 2008; Hajiahmadi et al. 2016). Local ramp metering strategies make use of traffic measurements in the vicinity of a ramp to calculate suitable ramp metering values, and then signals are released on slip roads to control access to the main road. Much current interest is focused on the difficult challenge of comprehensive control of all or most of the ramps on a network. It is rec-

Communicated by M. Anisetti.

✉ Hua Cui
huacui1122@gmail.com

[1] School of Information Engineering, Chang'an University, Xi'an, China

ognized that RM can directly restricts the on-ramp vehicles to enter the main road and the average density immediately downstream of the on ramp. However, using ramp metering alone to control freeway traffic has limited performance if the demands from on ramps and the upstream main road are high because the collective behaviors of the drivers are not controlled after entering the freeway. Therefore, complementary to RM, other control strategies such as variable speed limits (VSL) (Muller et al. 2015; Chow et al. 2009; Li and Chow 2015; Lu et al. 2010) have been investigated to control the collective vehicle speed (or driver behavior) of main road traffic. VSL not only can improve safety and emissions, but also can improve traffic performance by increasing throughput and reducing time delay. To fully control the freeway traffic in practice, many literatures considered both VSL and RM (Chow et al. 2009; Li and Chow 2015; Lu et al. 2010), which are believed to be the two key tools influencing conditions on congested freeways. Their combined effect was also studied in reducing the risk of crash and improvement in operational parameters such as speeds and travel times. It showed by simulations in many literatures that traffic flow significantly improved with combined VSL and RM versus using each strategy alone (Li and Chow 2015; Lu et al. 2010; Park and Smith 2010).

On the other hand, with the development of intelligent transportation system (ITS) and information technology, the merging problem had been researched from traffic management viewpoint by giving vehicle and infrastructure some intelligence, and thus a more microscopic approach to manage the merging traffic at an individual vehicle level has been investigated under the case of autonomous and intelligent vehicles and infrastructure with communication systems (Park and Smith 2010; Shao et al. 2015; Abbas et al. 2013; Khoufi et al. 2014; Imai et al. 2014; Wang et al. 2013; Dimitrakopoulos 2011). Ones refer to these intelligent microscopic merging controls as a merging assistant problem. So far, all the merging assistant researches are based on the assumption that all vehicles are automated and equipped with communication system, and Internet of Vehicles enables vehicles to communicate with each other by vehicle-to-vehicle (V2V) communication as well as with roadside base station s by vehicle-to-infrastructure (V2I) communication. As a matter of fact, on-ramp merging area of highway is an accident-prone section first because the traffic on the main road is disarranged by the vehicles' merging on the ramp lane and second because there are some blind spots in the merging areas so that vehicles on ramp are not able to decelerate fast enough when the vehicles on main road decelerate at unexpectedly high rates. Consequently, merging areas in a highway require a good and tight coordination between car drivers within a short time while vehicles are driving at high velocity. Any driver misbehavior or error may result in a car accident. The best way to insure vehicle merge smoothly with a minimum disturbance in the highway traffic and avoid accidents is to keep drivers informed about safety risks and provide better awareness of traffic conditions. Thus, preceding car on main road can take correct decision in a timely manner so that spare sufficient gap to accommodate the vehicles coming behind from ramp lane. Clearly, V2V communication offering information exchange in timely manner may drastically help drivers to accomplish this task and avoid incidents. The methods presented in (Khoufi et al. 2014; Imai et al. 2014; Wang et al. 2013; Dimitrakopoulos 2011) are capable of warning drivers of near-accident situations to enhance drivers' awareness of general safety.

However, such situation of Internet of Vehicles era is not foreseen in the near future, especially in developing country, and manual vehicles rather than intelligent vehicles would be prevailing. Having no direct control over vehicles, merging assistant technology and safety driving assistant technology at present are based on the perception of the driving environment using sensors, e.g., imaging sensors, ultrasonic sensors, infrared sensors, and induction loops (Yuan et al. 2011; Gramaglia et al. 2013; Medina and Benekohal 2016). The ability to detect the possible conflict is fundamental for minimizing car accidents and improving the traffic flow in merging areas. However, ultrasonic sensors are not high in detection accuracy and can be easily blocked by vehicles. Infrared detection is subject to be effected by vehicles' heat. Induction loops are regarded as highly accurate and reliable, but need to be placed under pavement, thus damaging the pavement. Furthermore, in some abnormal environmental conditions, for example, in extreme climatic conditions, or on-ramp merging area of expressway, or the corner of the village crossroads, these sensors are very easy to lapse and might cause high false alarm rate or high rate of leakage alarm. This problem occurred due to modeling inductive loops as a point in the traffic lane with no lane length. As vehicles may not always decelerate to the same position throughout the lane, in some instances the vehicles would never trigger the inductive loop to signify their presence, failing to sense vehicle on ramp lane. Meanwhile, imaging sensors (video camera) have been widely used because of their high lateral resolution and low cost and easy maintenance, which provide much richer information in comparison with the inductive loop. In particular, with large-scale applications of video surveillance and the considerable achievements in computer technology, image processing, artificial intelligence and pattern recognition technology, extracting and analyzing visual information from traffic surveillance videos has gained a great amount of interest worldwide in monitoring, control and management of traffic (Yuan et al. 2011). However, extracting information from video sensors involves substantial amount of processing, and video sensors are very sensitive to the environment illumination, weather conditions, occlusion problems, shadow

effects, etc (Alvarez and Lopez 2011). Therefore, robust and accurate and rapid detection and tracking of moving objects is still challenging in the case of outdoor traffic video surveillance. Video-based merging assistant technology also suffers from aforementioned issues (Laird et al. 2013; Wu et al. 2008; Laird and Geers 2012; Sultan et al. 2006). With the aim of further improving the knowledge of the traffic state, Wu et al. (2008) recommended to explore alternative sensor modalities (i.e., replacing inductive loop with video camera) for RM. Research in Sultan et al. (2006) explored the possibility of combining video cameras with the RM strategy for on-ramp queue control. But the work in Wu et al. (2008); Sultan et al. (2006) did not give details on video detection, whereas an assumption was made that all vehicles were detected inside the sensing range of the video camera. However, as studied in Laird et al. (2013); Sultan et al. (2006), this assumption may not be applicable because cameras may not be able to detect all vehicles on the ramp lane due to some kind of reasons, like environment illumination, weather conditions, occlusion, and so on.

This paper aims to alleviate congestion and safety problems in merging areas by video-based assistant technology. To achieve this, several maneuvers are developed for vehicle detection and tracking to produce a merging assistant approach adaptive to different weather and illumination conditions. Correspondingly, a merging assistant system with higher robustness and accuracy would be described. The rest of this paper is organized as follows. A system overview is provided in Sect. 2. Developed warning algorithm in this paper is described in detail in Sect. 3, including feature point extraction, vehicle tracking, vehicle behavior analysis, vehicle velocity calculation, performance evaluation. Experimental results are given in Sect. 4. Section 5 contributes to the conclusions.

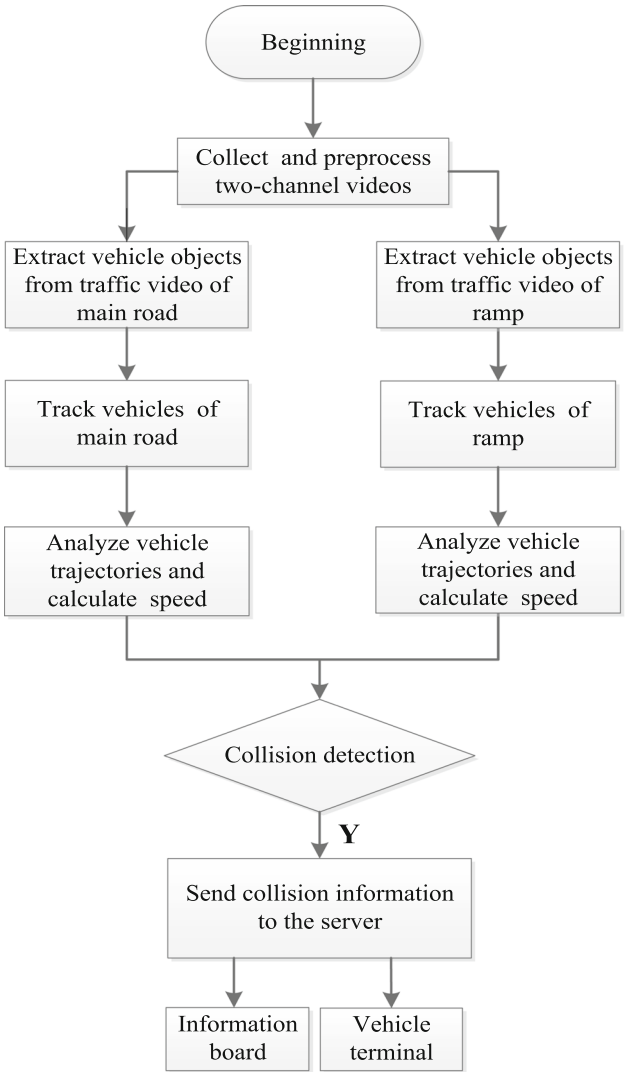

Fig. 1 Scheme of ramp warning system

2 System overview

The significance of active safety applications increases further in the ramp merging area where the visual line of sight is blocked by nearby buildings or objects. An active safety warning system is provided in this paper based on the dominant mono-camera with fixed height and viewing angle to capture the grayscale images. Figure 1 shows the scheme of this system. Figure 1 illustrates how to realize the collision detection and automatic warning to aid drivers to avoid possible collisions when two vehicles are approaching a ramp merging lane with a risk of collision. First step in flowchart is image preprocessing to reduce noise and eliminate wobble. Moreover, the regions of interest (ROI) would be set as shown in Fig 2. Considering the time spent by the communication system to deliver collision alarm message to the driver and by the driver to adjust the vehicle speed to pass merging zone safely, the end of the ROI should be set at a certain distance away from the merging zone. All following algorithms would be operated only in ROI for the purpose of reducing the calculation complexity. Second, the moving objects on ramp and main road would be extracted to make preparation for the vehicle tracking. Third, vehicle feature points extraction and tracking would be done, resulting in vehicle motion trajectories. Next, the position, velocity and direction of the target vehicle would be obtained by analyzing vehicle motion trajectories. Finally, through calculating the arriving time difference at ramp merging area between the on-ramp vehicle and main road vehicle, their collision risk grade is assessed, and corresponding warning message would be release to involved drivers by the means of roadside information board, vehicle terminal and mobile phone, etc. As the result, the drivers approaching ramp merging area would be aware that there is a vehicle coming from on-ramp or main road and what their collision risk is, then the main

Fig. 2 Configuration of ROI on the major road and the entrance ramp. **a** ROI on the main road. **b** ROI on the ramp

road vehicles may change lane to the inner lane or decelerate to make gap for the on-ramp vehicle, realizing the smooth and safe merging into the main road and avoiding the potential collision.

3 Ramp warning algorithm

In this section, the main steps of proposed active safety warning algorithm for the ramp merging areas will be described in detail following the procedure as shown in Fig. 1.

3.1 Vehicle object extraction

Frame difference method (Ki and Lee 2007) is one of widely used moving target detection methods and considers last frame image as background model rather than establishing background model, thus having the advantage of good real-time property and not sensitive to slow changing illumination. Therefore, it is adopted here to extract the moving vehicles from the monitoring videos of on-lamp and main road. However, objects extracted by traditional frame difference method always are a little bit bigger than actual ones. In order to obtain more satisfactory vehicle contour than traditional frame difference method, an improved method is developed and illustrated in Fig. 3. A frame difference image is written as $g_1(k) = |f(k+1) - f(k)|$ or $g_2(k) = |f(k) - f(k+1)|$ where $f(k)$ denotes the kth frame of traffic monitoring videos. And then the frame difference images $g_1(k)$ and $g_2(k)$ are processed by morphological dilation. $g(k)$ represents the intersection of two frame difference images, i.e., $g(k) = g_1(k) \cap g_2(k)$. Figure 4 shows the vehicle extraction result using the improved frame difference method.

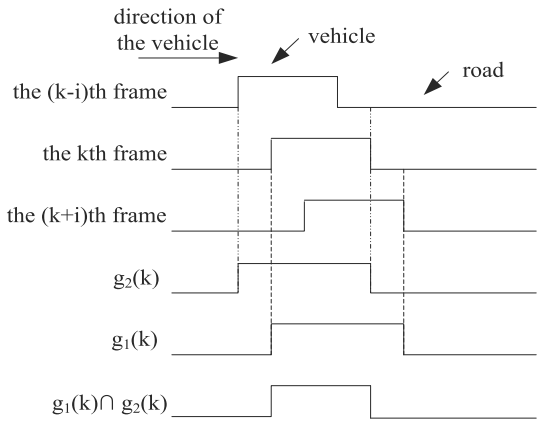

Fig. 3 Improved frame difference method

3.2 Vehicle tracking

Moving vehicle tracking algorithms available consider the whole vehicle or points on vehicles for tracking. The former is based on accurate segmentation for moving vehicles or modeling vehicle (Buch et al. 2011; Melo et al. 2006). However, many problems, e.g., illumination variations, shadow effects, vehicle overlapping, and bad weather conditions, will make the vehicle segmentation difficult to handle (Alvarez and Lopez 2011). Meanwhile, the high-level vehicle modeling algorithms always involve complex computation, which in turn is mostly unstable and time consuming. On the other hand, tracking points on vehicle can avoid vehicle segmentation and have the advantage of efficient locating and easy tracking (Kanhere and Birchfield 2008). So, we make an effort to select the most common low-level feature points on vehicles for tracking, and to modify the point tracking algorithm available to achieve better real-time tracking and more reliable tracking.

The vehicle corners in the video frames need to be detected before tracking vehicle. The improved Moravec detector (Schmid et al. 2000) is used to fulfill this task. The Moravec detector calculates the sum of squared differences (SSD) between a detected pixel and its adjacent pixels in the horizontal, vertical and diagonal directions. Commonly, vehicle corners on its surface can keep their relative positions stable over time, thus providing coherent motion information

(a) **(b)**

Fig. 4 Moving objects extraction by improved frame difference method. **a** Current traffic video frame. **b** Result of object extraction on the main road

of the vehicle during successive frames. However, Moravec detector tends to extract pseudo-corner-points formed by background scenes, which is extremely unfavorable for stable vehicle tracking. To circumvent this problem, the concept of image patch is introduced to the Moravec detector. Moreover, with the aim of the real-time warning, the sum of absolute differences (SAD) (Li and Tang 2013) instead of SSD metric is adopted to reduce computation burden. SAD measures the difference in the detected pixel (x, y) from surrounding image patches. Four SAD values corresponding to four directions, i.e., number 1, 2, 3 and 4 in Fig. 5, are obtained by formulas (1)–(4), and the smallest one is regarded as the eigenvalue $V(x, y)$ as expressed by formula (5). If the eigenvalue of the center point (x, y) is greater than a threshold value T, this point is marked as a corner. Then, varying i and j, all pixel points in each frame image would be detected if or not they are corners. Here, $W \times H$ is the size of the image patch and $w = \text{int}(W/2)$, $h = \text{int}(H/2)$. It is found that using aforementioned corners extraction method, several corners may be detected on one vehicle and the distribution of corners is usually intensive in a partial region, which influence tracking accuracy and increase the calculation amount. Therefore, it is necessary and critical to select qualified corners which can keep their positions stable. First, all the corners are sorted in a descending order according to their eigenvalues, and they are denoted as $p(x_i, y_i)$, where i values from 1 to the total number of corners N. Second, the position distance L_j between $p(x_i, y_i)$ and $s(x_j, y_j)$ would be calculated, where $s(x_j, y_j)$ is the selected qualified corners and j values from 1 to the total number of selected corners m. If the minimum L_j for all j is bigger than threshold T', $p(x_i, y_i)$ is selected as a qualified corner $s(x_j, y_j)$. Thus, only one or a very small number of feature points would be picked out for a moving object.

$$\text{SAD}_1 = \sum_{a=-w}^{w} \sum_{b=-h}^{h} |g(x-i+a, y+b) - g(x+i+a, y+b)| \quad (1)$$

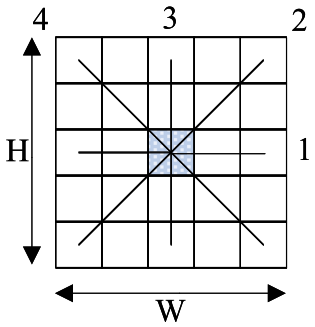

Fig. 5 Improved frame difference method

$$\text{SAD}_2 = \sum_{a=-w}^{w} \sum_{b=-h}^{h} |g(x-i+a, y-j+b) - g(x+i+a, y+j+b)| \quad (2)$$

$$\text{SAD}_3 = \sum_{a=-w}^{w} \sum_{b=-h}^{h} |g(x+a, y-j+b) - g(x+a, y+j+b)| \quad (3)$$

$$\text{SAD}_4 = \sum_{a=-w}^{w} \sum_{b=-h}^{h} |g(x+i+a, y-j+b) - g(x-i+a, y+j+b)| \quad (4)$$

$$V(x, y) = \min\{\text{SAD}_1, \text{SAD}_2, \text{SAD}_3, \text{SAD}_4\}. \quad (5)$$

Next, to track corresponding feature point on a vehicle in each video frame, a searching area around the feature point in the current frame and a matching template area around the corner in the previous frame are established. Then, a full search matching is carried out with the searching area and matching template. To reduce searching range and calculating amount, the feature point will be predicted by Kalman filter by considering that vehicle motion can be treated as uniform linear motions between two consecutive frames. Finally, we will get the motion trajectory of every feature point, while irregular track trajectories are removed. For details of our proposed tracking procedure, please see our

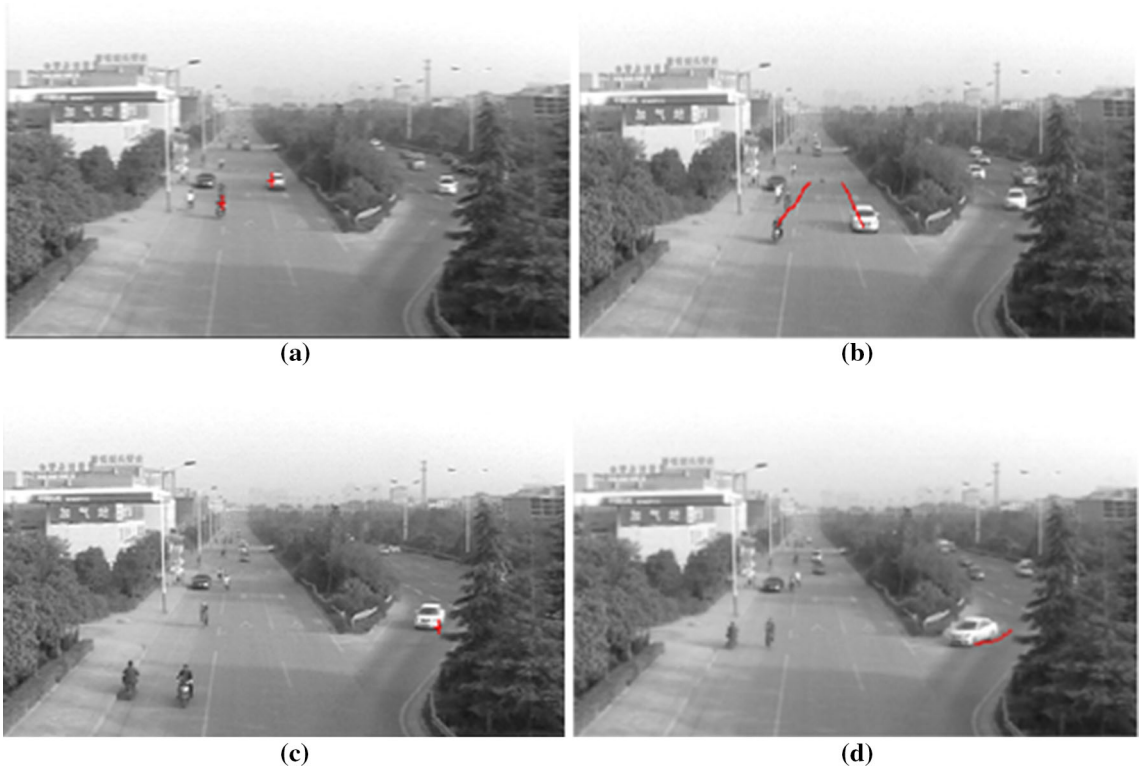

Fig. 6 Feature point extraction and vehicle tracking. **a** Feature point of vehicles on main road. **b** On-main road vehicle trajectories. **c** Feature point of vehicles on the ramp. **d** On-ramp vehicle trajectories

recent works presented in Song et al. (2014). Therefore, the moving vehicles are successfully tracked and their trajectories are obtained by our feature-point-based tracking method. The results are shown in Fig. 6. Then, clustering analysis is used to classify each trajectory into different vehicles. Firstly, feature points are transformed into the world coordinates in the zero height plane by inverse-projecting method and clustered into different classifications by K-means method. Then, 3D information of feature points can be estimated by using the relation between their velocities and heights and are matched with the given 3D vehicles models to delete and reassign feature points. Finally, the motion constraints of 3D trajectories are considered to recognize whether the trajectories belong to the same vehicle.

3.3 Assessment of collision risk grade

On the basis of the behavior analysis of moving vehicle trajectories, next we will calculate the vehicle velocity on the ramp and main road to define the collision risk grade.

3.3.1 Vehicle velocity estimation

The vehicle velocity is determined by the motion distance and motion time of a vehicle, and it can be analyzed in two parts. The first part is the coordinate transformation between the world coordinate system and the image coordinate system which is accomplished by distance-to-pixel mapping table. The second part is the calculation of real motion distance. To obtain more accurate distance, we need an appropriate calibration method to create a mapping table.

Camera calibration

Camera calibration is used to determine the mapping of world coordinates and image plane. Camera calibration is a basic and important issue due to the fact that its quality directly affects the accuracy and speed of the subsequent calculation of the vehicle velocity. There exist several camera calibration methods which can be divided into two categories, i.e., traditional calibration technique (Bas and Crisman 1997; Lenz and Tsai 1998) and self-calibration technique (Luong and Faugeras 1997; Pollefeys et al. 1998). The former depends on the particular reference object in various application scenes to get the mapping relation of the real space with the image. This kind of methods has simple algorithm and high accuracy. The latter uses the corresponding relation of the objects in the different frames to realize calibration. Such methods are much more flexible than the former because of its independence on the reference objects, but they are of lower accuracy. In this paper, aiming the high accuracy and fast speed warning, we prefer the former cal-

Fig. 7 Calibration with pavement marks. **a** Illustration for calibration method. **b** Reference marks on the ramp

ibration to calculate the speed of the target in the scene. Furthermore, with the prior knowledge of lane widths and pavement markings, this paper improves the traditional linear geometry calibration method. Our calibration method need not consider intrinsic parameters matrix of the camera and can yield the pixel-to-distance mapping table with relatively high accuracy and fast speed.

As shown in Fig. 7a, the labeled points A, B, E and F in the image denote the endpoints of pavement markings, and a and b label the two lane lines. Given that the distance between two adjacent points on the same lane line is 1500 cm, and the distance between two adjacent parallel lane lines is 375 cm. The image coordinates of any pixel on lane line a are known in advance, while A, B, E, and F are (x_1, y_1), (x_2, y_2), and (x_3, y_3), respectively. Suppose that the actual distance of the bottom pixel of the straight a is zero, and any point on the same straight in the image has the same distance. Given that the A and E have the same distance in the world coordinate system, all pixels on the straight AE thus have the same distances. The same is true for B and F. Therefore, the calibration is transformed to calculate the coordinates (x, y) of point Q on the lane line b with the same actual distance to any point $P(x_5, y_5)$ on the straight AB. Thus, Eq. $\frac{\mathrm{BP}}{\mathrm{BA}} = \frac{\mathrm{FQ}}{\mathrm{FE}}$ is true based on the linear model of camera calibration. Using four-point coordinates, we have

$$\frac{\mathrm{BP}}{\mathrm{BA}} = \frac{y_2 - y_5}{y_2 - y_1} = \frac{x_2 - x_5}{x_2 - x_1} \tag{6}$$

$$\frac{\mathrm{FQ}}{\mathrm{FE}} = \frac{y_4 - y}{y_4 - y_3} = \frac{x_4 - x}{x_4 - x_3}. \tag{7}$$

Substituting (6) and (7) into Eq. $\frac{\mathrm{BP}}{\mathrm{BA}} = \frac{\mathrm{FQ}}{\mathrm{FE}}$, we have

$$\begin{cases} \dfrac{y_2 - y_5}{y_2 - y_1} = \dfrac{y_4 - y}{y_4 - y_3} \\ \dfrac{x_2 - x_5}{x_2 - x_1} = \dfrac{x_4 - x}{x_4 - x_3}, \end{cases} \tag{8}$$

Thus

$$\begin{cases} y = y_4 - \dfrac{(y_2 - y_5)(y_4 - y_3)}{y_2 - y_1} \\ x = x_4 - \dfrac{(x_2 - x_5)(x_4 - x_3)}{x_2 - x_1}. \end{cases} \tag{9}$$

So, all points on the straight PQ possess the same actual distance with point P, while the actual distance of any point P can be easily obtained by one-dimensional linear calibration based on the geometrical prospective relationship of camera and three marking endpoints on lane line a. Let P traverse the straight AB, and one can follow Eq. (9) to obtain the mapping table which stores the actual distance of each pixel in the image patch ABEF and even in the whole image.

However, there usually exist some pixels which do not belong to any straight PQ, thus leading to no distance value in the mapping table. If these blank points are allowed, the accuracy of the mapping table will drop, causing the big error in the subsequent velocity calculation. So, the blank points should be given the appropriate distance values. This paper completes the mapping table in a simple way as follows. As shown in Fig. 8a, (x_1, y_1), (x_2, y_2), (x, y) are the image coordinates of pixels A, B and C, respectively. C is a blank point. A and B are not the blank points with actual distance value a and b, respectively. The points A and B are on the same column with C and most close to C. Then, the actual distance value c of point C can be calculated by Eq. (10).

$$c = \frac{b - a}{y_2 - y_1}(y - y_1) + a. \tag{10}$$

Therefore, implementing Eq. (10) on all the blank points, a complete mapping table is obtained. Moreover, with the increasing distances away from the camera of the pixels on the same column in the image, the actual distances in the mapping table should increase smoothly, whereas there exist some jump points in the mapping table, like B in Fig. 8b.

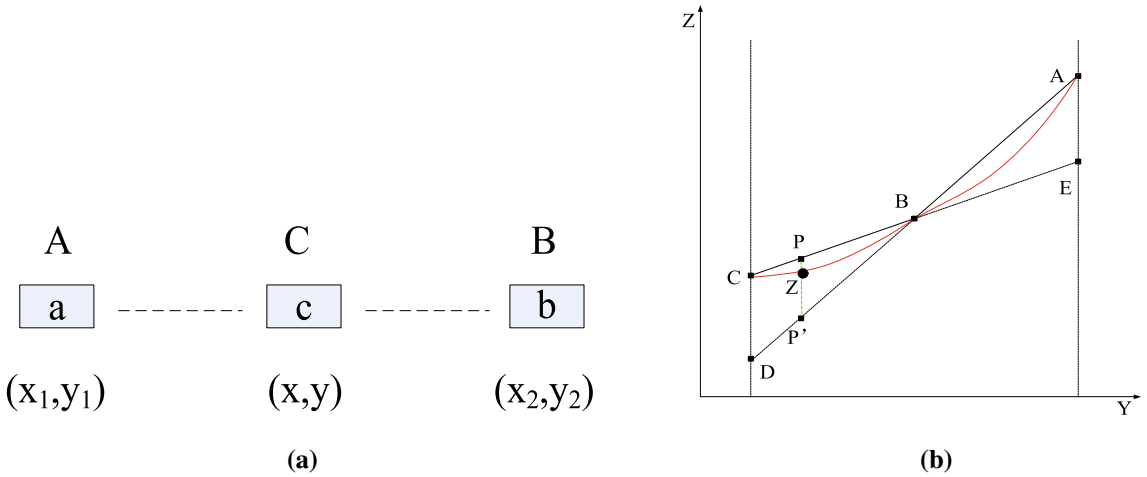

Fig. 8 Post-processing of mapping table. **a** Data completion. **b** Data smoothing

Therefore, data smoothing in the mapping table is expected to achieve much more accurate velocity. As shown in Fig. 8b, AB and BC have the same pixel distance in Y orientation, but have different slope. P is the arbitrary point on straight line BC, and P' on the AD has the same coordinates x and y to P, but different z, i.e., p and p_1, respectively. The smoothed z' value can be written as

$$z' = \frac{y_A - y_P}{y_A - y_C} \times p + \frac{y_P - y_C}{y_A - y_C} \times p_1, \tag{11}$$

where y_A is the Y coordinate of point A. In Fig. 8b, the curve through the point Z is the smoothing result.

Vehicle velocity estimate

Figure 9 is the diagram of a merging area scenario. As shown in Fig. 9, two cameras are set up on the pole which locates at the main road near the crossing. One is used to shoot video for the main road and the other for the ramp. Next, this paper estimates the velocity of a vehicle on the main road and ramp by using the trajectory and mapping table. Since our interest is whether vehicles can pass the merging zone safely, we only estimate the velocities of the certain vehicles on the main road which are heading toward the merging zone and ignore the moving vehicles toward the opposite direction. Therefore, we must detect the vehicles which are already on the side lane and are meant to change to the side lane. In the other hand, all the vehicles on the ramp are considered, because the ramp usually is one way. Consequently, there is no need to judge the moving direction of the vehicles on the ramp and which lane they are on.

Looking up our mapping table established in 3.3.1(1) is the way to transform the pixel coordinates into the world distances. The same is true for the feature points on the vehicle trajectory produced by the method presented in Sect. 3.2. Thus, the actual distance of the feature points can be known. For the feature point sequences with respect to the time, if the corresponding distance values decrease, we can tell the vehicle is coming toward the merging zone. Then, we selected a side-lane boundary as the benchmark lane line. Then, the distance between the benchmark lane line and the trajectory is defined as (12), where (x_{Ti}, y_{Ti}) is the pixel of the trajectory in the row i, (x_{Li}, y_{Li}) is the pixel of the benchmark lane line, and N is the number of the tracking frames. When the value of the D is within the thresholds which have been set based on the priori knowledge, it indicates that the vehicle is on the side lane or meant to change to side lane.

$$D = \frac{\sum_{i=0}^{N}(x_{Ti} - x_{Li})}{N}. \tag{12}$$

For the vehicles on the main road and ramp which satisfy the requirements mentioned above, next we calculate their velocities. Because the velocity of a vehicle could not change greatly during a short time, one can think its speed is uniform. Therefore, for the not too long detection region, the estimate of the vehicle velocity is derived as formula (13).

$$V = \frac{|S' - S|v}{p - q}, \tag{13}$$

$|S' - S|$ denotes the distance between the vehicle positions in the frame p and q. S' and S are obtained by looking up the mapping table of two channel videos. v is the video speed. V represents the speed of a vehicle at the time of frame k ($q \leq k < p$). A series of experiments show the velocity estimated by (13) is very accurate with the absolute error of no more than 1.5% compared to that by radar-based method.

3.3.2 Collision risk grade

Based on the detected position and velocity of a vehicle on the main road or ramp, one can estimate their entrance times

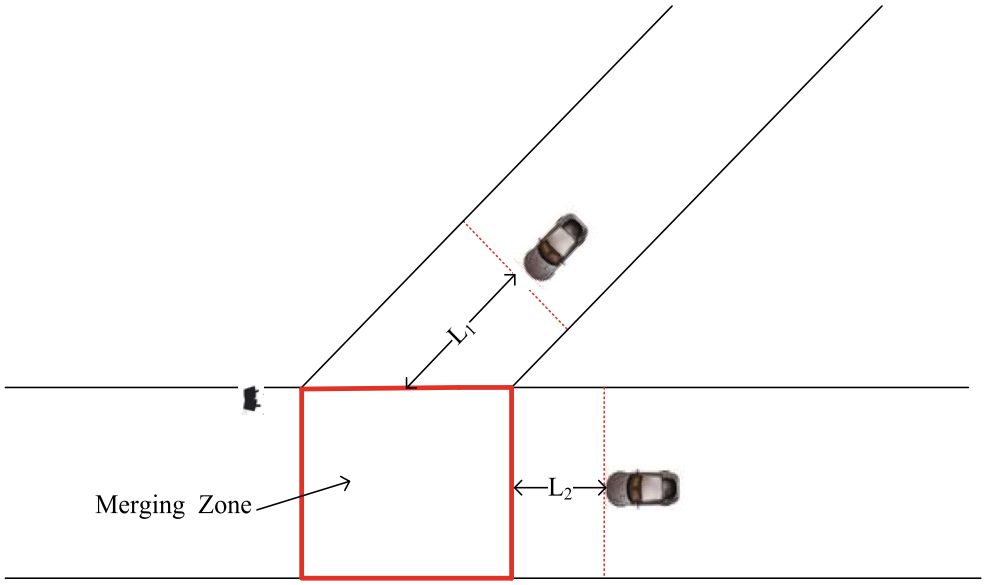

Fig. 9 Diagram of merging area

into the merging zone. Subsequently, the arrival time lag t between the two vehicles which touch the border of merging zone on the ramp and the main road could be calculated by formulas (14).

$$t = \left| \frac{L_1 + S'_{kR}}{V_{kR}} - \frac{L_2 + S'_{hM}}{V_{hM}} \right|. \tag{14}$$

V_{kR} is the speed of the on-ramp vehicle at the time of frame k, and V_{jM} the speed of on-main-road vehicle at the time of frame h. And S'_{kR} and S'_{hM} are the actual distances corresponding to vehicle positions in the frame k of ramp video and in the frame h of main road video, respectively. As shown in Fig. 9, L_1 and L_2 are the distance of the merging zone from the end of the ROI region on the ramp and main road, respectively.

According to the lag t, we determine risk grades, as described by formula (15). The risk grade is assumed to be A, when t is less than t_1. That is to say, if two drivers keep the current speeds, a collision will be likely to occur. So they must be highly vigilant for their driving behavior and take measures to avoid collision. For example, one vehicle stops to yield to other vehicle. When t is between t_1 and t_2, the risk grade is denoted by B, implying drivers have enough time to adjust their speed so that both vehicles pass the merging zone safely. When t is bigger than t_2, the risk grade is C, denoting this case will be safe for vehicles from both directions. The thresholds are set according to the special road type.

$$t = \begin{cases} A & t < t_1 \\ B & t_2 < t < t_3 \\ C & t > t_3. \end{cases} \tag{15}$$

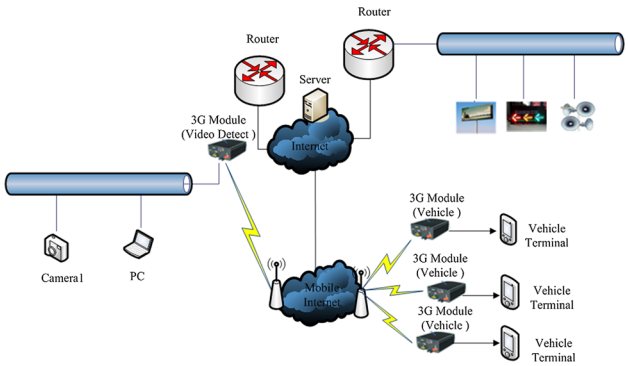

Fig. 10 The release of the collision alarm

3.3.3 Warning information release

The automatic warning is very important to improve driving efficiency and security. It is established on the basis of information exchange between human, vehicles and roads. A variety of state-of-the-art technologies of wireless sensor networks and wireless communication technology (Martinez 2010) are used, such as RFID, Wi-Fi, WAVE, and 3G. In this paper, we adopt the 3G technology (Lampropoulos et al. 2010) which is based on WWAN (wireless wide area network). Once there is the collision information, the server will send it to information board and vehicle terminal using the 3G technology, as shown in Fig. 10. The collision warning information is released on the information board, where Red denotes that the collision risk grade of the two cars which are located at red squares is A, and Blue illustrates that the current risk grade of the two cars which are located at blue squares is B, and Green denotes that the risk grade of the two cars which are located at green squares is C.

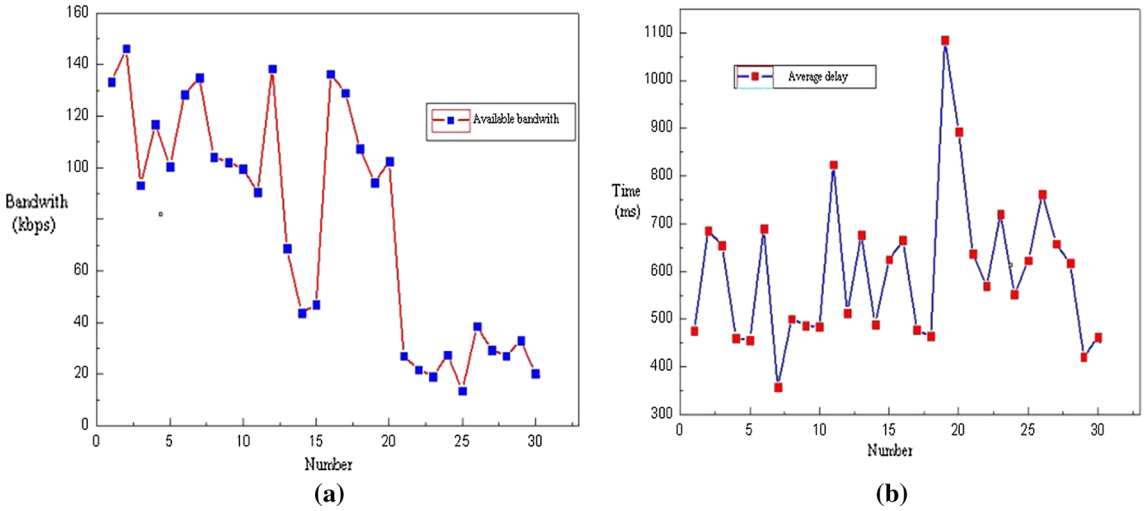

Fig. 11 Network bandwidth available and average delay. **a** Bandwidth available. **b** Average delay

Table 1 Part data in the pixel-to-distance mapping stable

Row	Column												
	354	355	356	357	358	359	360	361	362	363	364	365	366
136	3089	3089	3089	3089	3146	3146	3146	3146	3204	3204	3204	3204	3264
135	3032	3032	3032	3032	3089	3089	3089	3089	3146	3146	3146	3146	3204
134	2976	2976	2976	2976	3032	3032	3032	3032	3089	3089	3089	3089	3146
133	2922	2922	2922	2922	2976	2976	2976	2976	3032	3032	3032	3032	3089
132	2869	2869	2869	2869	2922	2922	2922	2922	2976	2976	2976	2976	3032
131	2817	2817	2817	2817	2869	2869	2869	2869	2922	2922	2922	2922	2976
130	2767	2767	2767	2767	2817	2817	2817	2817	2869	2869	2869	2869	2922
129	2718	2718	2718	2718	2767	2767	2767	2767	2817	2817	2817	2817	2869
128	2670	2670	2670	2670	2718	2718	2718	2718	2767	2767	2767	2767	2817
127	2623	2623	2623	2623	2670	2670	2670	2670	2718	2718	2718	2718	2767
126	2577	2577	2577	2577	2623	2623	2623	2623	2670	2670	2670	2670	2718
125	2532	2532	2532	2532	2577	2577	2577	2577	2623	2623	2623	2623	2670
124	2488	2488	2488	2488	2532	2532	2532	2532	2577	2577	2577	2577	2623
123	2446	2446	2446	2446	2488	2488	2488	2488	2532	2532	2532	2532	2577
122	2404	2404	2404	2404	2446	2446	2446	2446	2488	2488	2488	2488	2532
121	2363	2363	2363	2363	2404	2404	2404	2404	2446	2446	2446	2446	2488
120	2323	2323	2323	2323	2363	2363	2363	2363	2404	2404	2404	2404	2446
119	2283	2283	2283	2283	2323	2323	2323	2323	2363	2363	2363	2363	2404
118	2245	2245	2245	2245	2283	2283	2283	2283	2323	2323	2323	2323	2363
117	2207	2207	2207	2207	2245	2245	2245	2245	2283	2283	2283	2283	2323
116	2170	2170	2170	2170	2207	2207	2207	2207	2245	2245	2245	2245	2283
115	2134	2134	2134	2134	2170	2170	2170	2170	2207	2207	2207	2207	2245
114	2098	2098	2098	2098	2134	2134	2134	2134	2170	2170	2170	2170	2207

4 Experiments

Table 1 lists the part data of the pixel-to-distance mapping table corresponding to the image of size 720×288 in Fig. 7a. A series of experiments show the mapping table is of accuracy with absolute error of no more than 1%. For example, d_{ji} is used to denote the distance between point J and I, and d_{kj} the distance between K and J. Point I, J and K are the marking ends corresponding to the start of lane line b, E and Q, respectively. By looking up the mapping table, we know

Table 2 Experiment results in various scenarios

Scenario no.	Early warning times	Observations	Warning accuracy
1	424	414	97.6%
2	518	508	98.1%
3	492	482	98.0%
4	379	373	98.4%

$d_{ji} = 1656 - 145 = 1511$, $d_{kj} = 3146 - 1656 = 1490$. The comparison of such values with the real distance 1500 cm shows the absolute error is about 0.1%The high accurate mapping table ensures the accuracy of the velocity estimation.

The system was tested with the vehicle speed range from 30 km/h to 80 km/h in Xian of China. The information release rate was evaluated by software Qcheck which measures transmission speed from the Internet to vehicle terminal. Here, the measurement interval was one minute, and our communication system sends warning information three times to get the minimum, maximum and average transmission delay. Figure 11 shows the detection results for various vehicles speeds on main road and ramp. The bandwidth available is from 15 kbps to 150 bps, and the delay ranges from 350 ms to 1100 ms, and the dropping packer ratio is about 3%, which indicates that the proposed warning system has high performance and good robustness.

The warning system was implemented in four merging zones during one week on the freeway with large traffic in Xian city. From the test results listed in Table 2, we can see the correct warning rate is up to 98% for various scenarios. In addition, the proposed warning system just needs 1 s to make drivers achieve warning information after entering the detection region.

5 Conclusions

A real-time early ramp warning technology is proposed in this paper based on the analysis of vehicle trajectories. In order to reduce the computation time and ensure the real-time performance, many methods in the processing procedure are improved. Firstly, the frame difference method for vehicle extraction and Moravec algorithm for feature point extraction are improved. Then, vehicle trajectories can be obtained by tracking the feature points with a specially designed template in the image sequences. Secondly, improved calibration method is proposed. Finally, the risk grades are defined and then released to drivers by the vehicle terminal and information board. Experimental results show that this warning system can make drivers aware of the potential collision in advance. In addition, it is not restricted by environment and could release real-time and reliable warning information with easy realization and high accuracy within the scope of all vehicles.

Acknowledgements The authors acknowledge the support of the National Natural Science Foundation of China (No. 61572083), the Natural Science Foundation of Shaanxi Province (No.2015JQ6230), and the Special Fund for Basic Scientific Research of Central Colleges (No.310824152009). They furthermore thank the anonymous reviewers for valuable comments

Compliance with ethical standards

Conflict of interest All authors declare that they have no conflict of interest.

Ethical approval This article does not contain any studies with human participants or animals performed by any of the authors.

References

Abbas T, Bernado L, Thiel A, Mecklenbruker CF, Tufvesson F (2013) Measurements based channel characterization for vehicle-to-vehicle communications at merging lanes on highway. In: In proceedings of the 5th international symposium wireless vehicular communications, IEEE, pp 1–5

Alvarez JMA, Lopez AM (2011) Road detection based on illuminant invariance. IEEE Trans Intell Transp Syst 12(1):184–193

Bas EK, Crisman JD (1997) An easy to install camera calibration for traffic monitoring. In: In proceedings of the IEEE international conference on intellegent transportation systems, pp 362–366

Bertini RL, Malik S (2004) Observed dynamic traffic features on freeway section with merges and diverges. Transp Res Rec 1867:25–35

Buch N, Velastin SA, Orwell J (2011) A review of computer vision techniques for the analysis of urban traffic. IEEE Trans Intell Transp Syst 12(3):920–939

Chow AHF, Lu XY, Qiu ZJ, Shladover S, Yeo H (2009) An empirical study of traffic breakdown for variable speed limit and ramp metering control. In: 89th TRB Annual Meeting, pp 10–14

Dimitrakopoulos G (2011) Intelligent transportation systems based on internet-connected vehicles: fundamental research areas and challenges. In: 11th international conference on ITS telecommunications (ITST), August 2011, pp 145–151

Gramaglia M, Bernardos CJ, Calderon M (2013) Virtual induction loops based on cooperative vehicular communications. Sensors 13(2):14671476

Hajiahmadi M, Van dWGS, Tampere C, Corthout R (2016) Integrated predictive control of freeway networks using the extended link transmission model. IEEE Tran Intell Transp Syst 17(1):6578

Imai S, Taguchi K, Kashiwa T (2014) Effect of positions of car antenna on radio wave propagation for inter-vehicle communications at intersection. In: IEICE Technical report, EST2014-40, p 187190

Janson BN, Awad W, Robles J, Kononov J, Pinkerton B (1998) Truck accidents at freeway ramps: data analysis and high-risk site identification. J Transp Stat 1:75–92

Kanhere NK, Birchfield ST (2008) Real-time incremental segmentation and tracking of vehicles at low camera angles using stable features. IEEE Trans Intell Transp Syst 9(1):148–160

Khoufi I, Laouiti A, Wehbi B (2014) Tar channel access mechanism: a study of a highway ramp car merge case. In: International conference on new technologies, mobility and security, pp 1–5

Ki YK, Lee DY (2007) A traffic accident recording and reporting model at intersections. IEEE Trans Intell Transp Syst 8(1):1–7

Laird J, Geers DG (2012) Modeling impact of sensor placement for vision-based traffic monitoring. Transp Res Rec J Transp Res Board 2315:110–120

Laird J, Geers DG, Wang Y, Chou CT (2013) Integrating video cameras for alinea on-ramp queue length estimation. In: Proceedings of the 16th international IEEE annual conference on intelligent transportation systems, The Hague, The Netherlands, 6-9 Oct 2013, pp 1571 – 1578

Lampropoulos G, Skianis C, Neves P (2010) Optimized fusion of heterogeneous wireless networks based on media independent handover operations. IEEE Wirel CommunMag 17(4):7887

Lenz RK, Tsai RY (1998) Techniques for calibration of the scale factor and image center for high accuracy 3d machine vision metrology. IEEE Trans PAMI 10(5):713–720

Li Y, Chow A (2015) Optimisation of motorway operations via ramp metering and variable speed limits. Transp Plan Technol 38(1):94–110

Li P, Tang H (2013) A low-power vlsi implementation for fast full-search variable block size motion estimation. Int J Electron 100(9):1240–1255

Lu XY, Varaiya P, Horowitz R, Su D, Shladover SE (2010) A new approach for combined freeway variable speed limits and coordinated ramp metering. In: 13th international IEEE annual conference on intelligent transportation systems, Madeira Island, Portugal, 19-22 Sept 2010, pp 491–498

Luong QT, Faugeras O (1997) Self-calibration of a moving camera from point correspondences and fundamental matrices. Int J Comput Vis 22(3):261–289

Martinez FJ (2010) Emergency services in future intelligent transportation systems based on vehicular communication networks. IEEE Intell Transp Syst Mag 2(2):620

Medina J, Benekohal R (2016) Microwave radar vehicle detection performance at railroad grade crossings with quad gates in normal and adverse weather conditions. Transp Res Rec J Transp Res Board 2545(2545):123–130

Melo J, Naftel A, Bernardino A, Santos-Victor J (2006) Detection and classication of highway lanes using vehicle motion trajectories. IEEE Trans Intell Transp Syst 7(2):188200

Muller ER, Carlson RC, Kraus W, Papageorgiou M (2015) Microsimulation analysis of practical aspects of traffic control with variable speed limits. IEEE Trans Intell Transp Syst 16(1):1–12

Papageorgiou M, Kotsialos A (2002) Freeway ramp metering: an overview. IEEE Trans Intell Transp Syst 3(4):271–281

Papageorgiou M, Papamichail I (2008) Overview of traffic signal operation policies for ramp metering. TRB Transp Res Rec 2047:28–36

Park H, Smith BE (2010) Investigating benefits of intelligent-drive in freeway operations—lane changing advisory case study. In: In the 89th annual meeting of the transportation research board, Washington D.C

Pollefeys M, Van Gool L, Proesmans M (1998) Self-calibration and metric reconstruction in spite of varying and unknown internal camera parameters. In: Proceeding of International Conference on Computer Vision, pp 90–95

Schmid C, Mohr R, Bauckhage C (2000) Evaluation of interest point detectors. Int J Comput Vis 37(20):151–172

Shao C, Leng S, Zhang Y, Vinel A (2015) Performance analysis of connectivity probability and connectivity-aware mac protocol design for platoon-based vanets. IEEE Trans Veh Technol 64(12):5596–5609

Song H, Lu S, Ma X (2014) Vehicle behavior analysis using target motion trajectories. IEEE Trans Veh Technol 63(8):3580–3591

Sultan B, McDonald M, Wu J (2006) The benefit of video detection for onramp queue control and alinea ramp metering strategy. In: Traffic engineering and street management-practical applications of microsimulation

Wang Y, E W, Tang W, Tian D, Lu G, Yu G (2013) Automated on-ramp merging control algorithm based on internet-connected vehicles. IET Intell Transp Syst 7(4):371–379

Wu J, Jin X, Horowitz AJ (2008) Methodologies for estimating vehicle queue length at metered on-ramps. Transp Res Rec 2047(1):75–82

Yi HW, Mulinazzi TE (2007) Urban freeway on-ramps: Invasive influences on main-line operations. Transp Res Rec 2023:112–119

Yuan G, Zhang X, Yao QM (2011) Hierarchical and modular surveillance systems in its. IEEE Trans Intell Transp Syst 26(5):10–15

Zhang XD, Guo ZY, Gao JP, Jiang R (2006) Safety theory analysis of on-ramp merging area of expressway. J Chong Qing Traffic Inst 25(1):99–103